Molecular and Cellular Neuroscience **6**, 363–379 (1995)

MCN

Dynamics of MASH1 Expression *in Vitro* and *in Vivo* Suggest a Non-Stem Cell Site of MASH1 Action in the Olfactory Receptor Neuron Lineage

Melinda K. Gordon,* Jeffrey S. Mumm,* Rachel A. Davis,* J. David Holcomb,* and Anne L. Calof*,†,[1]

**Department of Biological Sciences, University of Iowa, Iowa City, Iowa 52242; and †Department of Anatomy and Neurobiology and Developmental Biology Center, University of California College of Medicine, Irvine, California 92717*

Disruption of the mouse gene encoding the transcription factor MASH1 leads to loss of certain classes of neurons, including receptor neurons of the olfactory epithelium (OE). Here we investigate the nature of the cell type expressing MASH1 in mouse OE by manipulating olfactory receptor neuron (ORN) neurogenesis *in vitro* and *in vivo* to alter the dynamics of neuronal production. The results indicate that MASH1 is expressed in cells of the ORN lineage, but not in ORNs themselves nor in their immediate precursors. Data on how changes in the numbers and proliferative states of MASH1$^+$ cells correlate with induced changes in overall neurogenesis strongly suggest that MASH1-expressing cells give rise to the immediate precursors of ORNs, but are not the self-renewing stem cells of the OE. The results imply that multiple progenitor stages are employed in generating ORNs and suggest that the action of MASH1 occurs predominantly at an intermediate stage.

INTRODUCTION

The genes that control neurogenesis—the proliferation of neural precursors and the production of postmitotic neurons—are poorly understood in higher vertebrates. Studies in invertebrates have identified both "neurogenic" genes, which act in cells at early stages to control epithelial versus neural determination, and "proneural" genes, which are required for the development of subsets of neuroblasts (for reviews, see Campos-Ortega and Jan, 1991; Campuzano and Modolell, 1992; Greenspan, 1992; Campos-Ortega, 1993). Recently, mammalian homologues of *Drosophila* proneural genes of the *achaete–scute* complex have been cloned; these include *Mash1* and *Mash2* (mammalian achaete–scute homologues 1 and 2), which encode basic helix–loop–helix transcription factors (Johnson *et al.*, 1990; Guillemot and Joyner, 1993). Although *Mash2* does not appear to play a role in nervous system development (Guillemot *et al.*, 1994), *Mash1* does appear to function in mammalian neurogenesis: MASH1 is expressed in regions of the mouse embryo where proliferating neural precursors are present (Lo *et al.*, 1991), and disruption of the *Mash1* gene in mice results in a profound reduction in the numbers of several types of neurons including autonomic, enteric, and olfactory receptor neurons (Guillemot *et al.*, 1993; Blaugrund *et al.*, 1994). These effects are accompanied by perinatal lethality.

Although these studies establish an important role for *Mash1* in vertebrate neurogenesis, they leave unanswered questions about the nature of the cells in which *Mash1* acts. For example, are certain neurons absent in *Mash1*$^{-/-}$ mice because *Mash1* gene expression is required at some particular stage in their development? If so, at what stage in a neuronal lineage is MASH1 required: in newly generated neurons themselves, in the immediate precursor of those neurons, in more distantly related progenitors, or perhaps even in self-renewing neural stem cells? This latter question is difficult to address for vertebrate neurons because the number of cellu-

[1] To whom correspondence should be addressed at Dept. of Anatomy and Neurobiology, 364 Med Surge II, University of California College of Medicine, Irvine, CA 92717-1275. Fax: (714) 824-1104. E-mail: alcalof@uci.edu.

1044-7431/95 $12.00

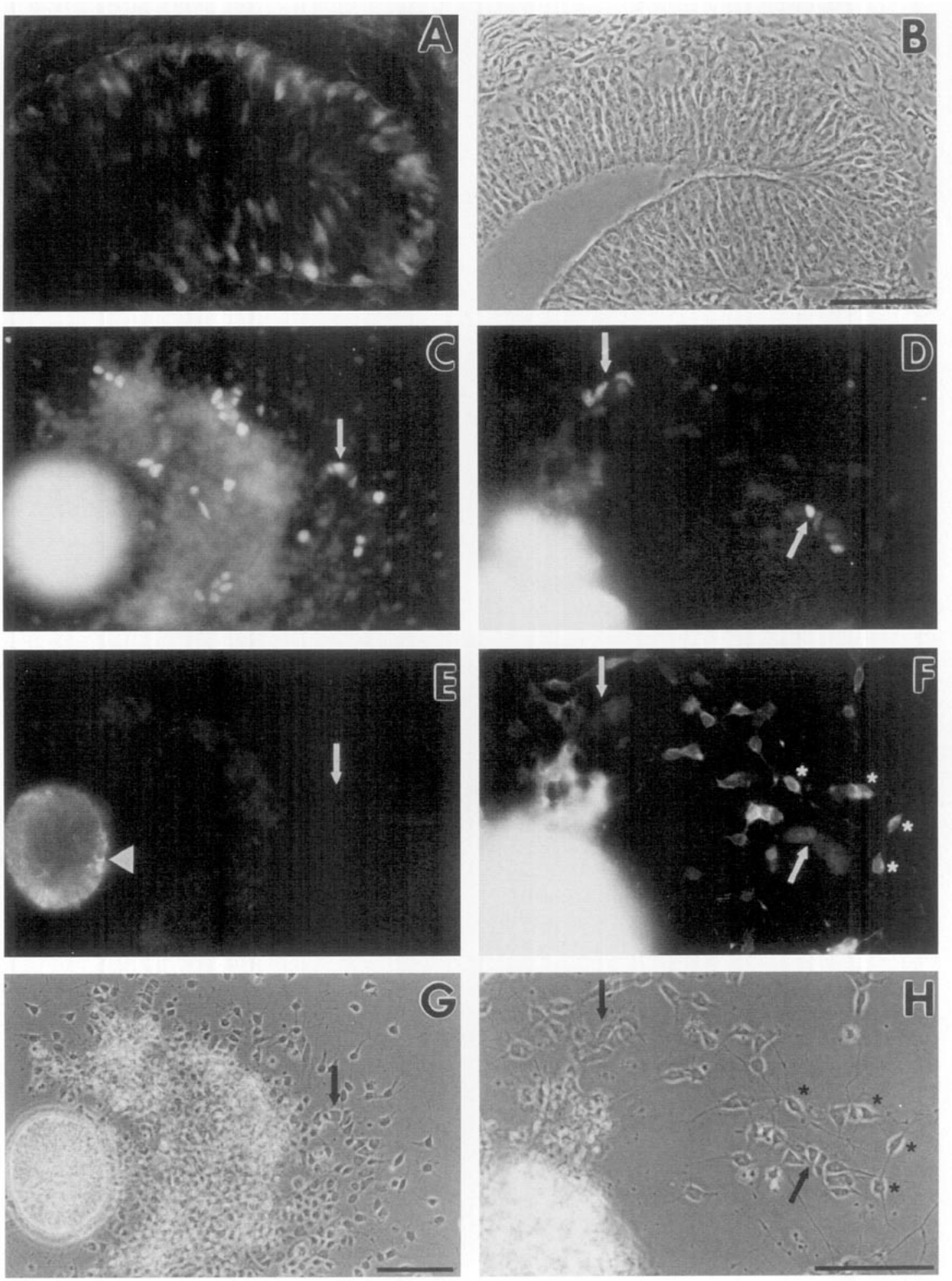

FIG. 1. Expression of MASH1 in cells of the OE *in vivo* and *in vitro*. (A–B) Twelve-micrometer cryostat sections of embryonic day 15.5 mouse OE were processed for MASH1 immunoreactivity. (A) Section through a developing nasal turbinate, viewed in rhodamine optics, shows that scattered MASH1$^+$ cells are present throughout the OE, particularly near the basal lamina. (B) Same field, viewed under phase-contrast optics,

TABLE 1
[^{3}H]TdR Labeling Index of MASH1-Expressing Cells in OE Explant

Time of fixation; [^{3}H]TdR pulse length	Percentage of migratory cells that are [^{3}H]TdR$^+$ (SD)	Percentage of migratory cells that are MASH1$^+$ (SD)	Percentage of [^{3}H]TdR$^+$ cells that are MASH1$^+$ (SD)	Percentage of MASH1$^+$ cells that are [^{3}H]TdR$^+$ (SD)	Percentage of migratory cells that are both MASH1$^+$ and [^{3}H]TdR$^+$ (SD)
t = 6 h	16.32	4.53	11.42	40.47	1.83
4- to 6-h pulse	(2.58)	(0.31)	(1.35)	(1.11)	(0.60)
t = 6 h	31.38	4.20	10.94	80.42	3.38
0- to 6-h pulse	(2.82)	(0.20)	(1.84)	(2.51)	(0.27)

Note. OE explant cultures were pulsed with [^{3}H]TdR for either 2 h (5 μCi/ml) or the entire 6-h culture period (1 μCi/ml). After fixation and processing for MASH1 immunoreactivity and autoradiography, the migratory cells surrounding OE explants were evaluated as follows: The total number of migratory cells surrounding the body of each explant was counted, and each migratory cell was evaluated for [^{3}H]TdR incorporation (silver grains over the nucleus) and MASH1 expression (brightly fluorescent nucleus under rhodamine optics; see Fig. 2). For each of the two [^{3}H]TdR labeling paradigms, 8–10 explants in two separate cultures, for a total of approximately 2000 migratory cells per culture, were evaluated.

lar stages required to give rise to a neuron is generally not known, nor in most cases is it necessary that true, self-renewing stem cells be involved (Calof, 1995).

To address these questions, we took advantage of the fact that one of the neuronal types depleted in *Mash1*$^{-/-}$ mice is the olfactory receptor neuron (ORN), a cell type uniquely suited for studies of neurogenesis. The tissue that produces ORNs, the olfactory epithelium (OE), is one of the few vertebrate tissues that generates neurons continuously throughout life (Graziadei and Monti Graziadei, 1978). This property makes it possible not only to observe but also to manipulate ORN neurogenesis in adults. For example, severing the contacts of ORNs with their synaptic target tissue, the olfactory bulb of the brain, leads to ORN death, followed by an increased rate of proliferation in the OE, followed in turn by the production of new ORNs (Monti Graziadei and Graziadei, 1979; Camara and Harding, 1984; Schwartz Levey *et al.*, 1991; Holcomb *et al.*, 1995). In addition, OE can be isolated in pure form from mouse embryos, and cultures can be established that undergo neurogenesis for at least several days (Calof and Chikaraishi, 1989; DeHamer *et al.*, 1994).

Analysis of embryonic OE cultures has already indicated that the immediate precursor of ORNs is not a stem cell, but rather a symmetrically dividing cell with a limited capacity for self-amplification that can be regulated by growth factors (DeHamer *et al.*, 1994). To date, markers that identify a neuronal stem cell in the OE have not been discovered, although the fact that this tissue undergoes continuous neuronal replacement suggests that, in this region of the nervous system at least, a stem cell almost certainly exists.

In the present study, we have observed and manipulated OE neurogenesis *in vitro* in tissue from mouse embryos and *in vivo* in adult mice in which neurogenesis has been induced by removal of the olfactory bulb (the synaptic target tissue of ORNs). We have analyzed the types, numbers, and proliferative states of cells that express MASH1 under both conditions. The data support the idea that MASH1-expressing cells are an early stage of neuronal progenitor cell in the OE and that they give rise to the immediate precursors of ORNs. However, the proliferative dynamics of MASH1-expressing cells suggest that they are not the stem cells in the ORN lineage. The results of these studies suggest that the action of *Mash1* in vertebrate nervous system development is intrinsic to specific neuronal lineages and provide insight into the stage at which *Mash1* action is likely to be re-

shows the entire epithelium and some of its underlying stroma. Bar, 50 μm. (C–H) Embryonic OE explants cultured for 10 h were fixed and processed for double-label immunofluorescence for MASH1 and keratin (C, E, G) or for MASH1 and N-CAM (D, F, H). (C) Rhodamine optics showing MASH1 immunoreactivity (arrow indicates MASH1-expressing cell). (D) Rhodamine optics of a different field, showing MASH1 immunoreactivity (arrows indicate MASH1-expressing cells). (E) The same field as in C viewed in fluorescein optics, showing keratin immunoreactivity (large arrowhead indicates keratin-expressing cells in the body of the explant, arrow indicates position of MASH1-expressing cell shown in C). (F) The same field as in D, viewed in fluorescein optics, showing N-CAM immunoreactivity (asterisks indicate N-CAM-expressing cells, arrows indicate positions of MASH1-expressing cells shown in D). (G) The same field as in C and E, viewed under phase-contrast optics (arrow indicates the MASH1-positive/keratin-negative cell shown in C and E. (H) The same field as in D and F viewed under phase-contrast optics (arrows indicate the Mash1-positive/N-CAM-negative cells shown in D and F, asterisks indicate the N-CAM-positive cells shown in F). Bars, 50 μm.

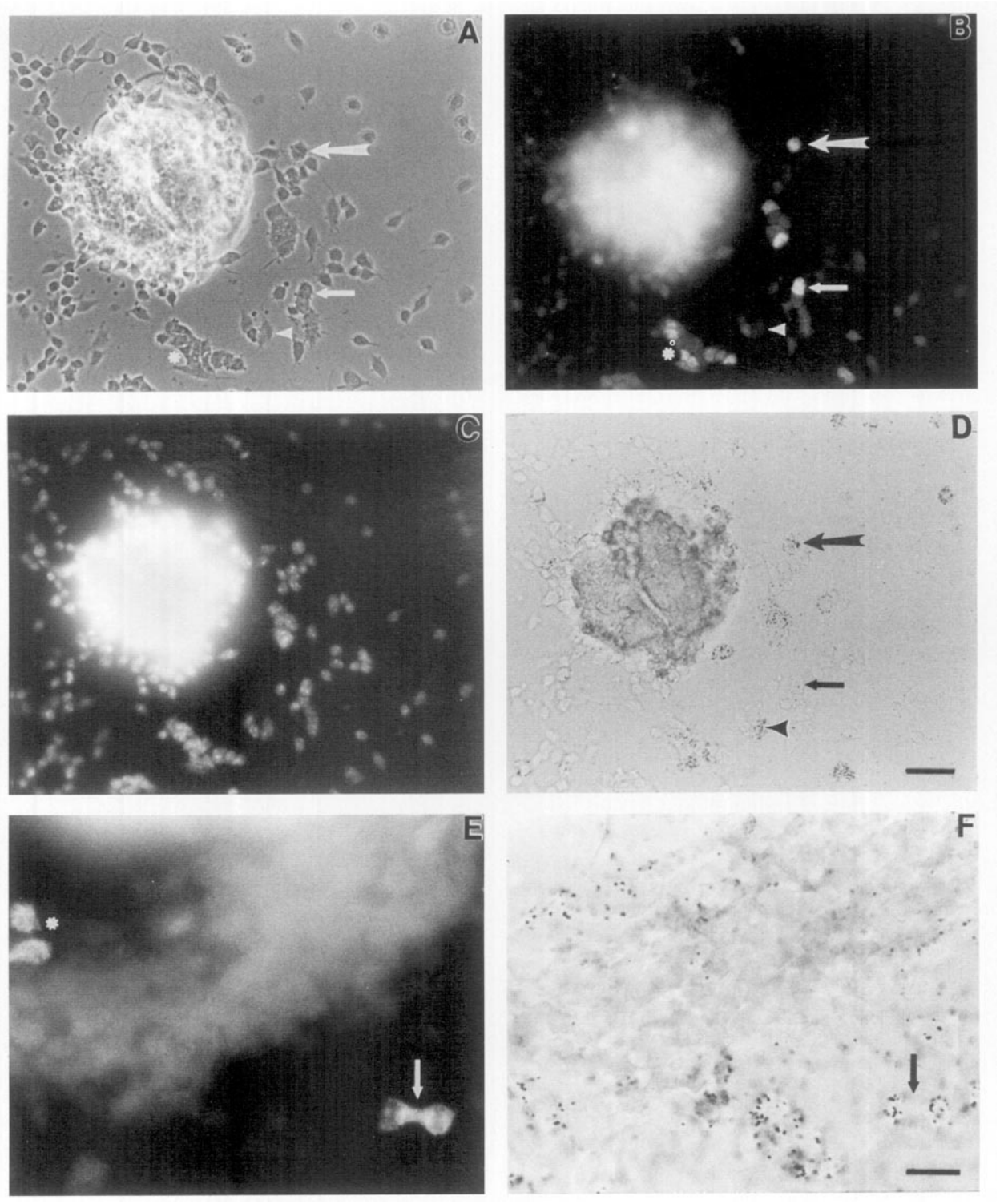

FIG. 2. MASH1 is expressed by a subpopulation of proliferating migratory cells in embryonic OE cultures. (A–D) OE explants were cultured *for 6 h, with* [^{3}H]TdR (5 μCi/ml) *added during the last 2 h, then fixed and processed for MASH1 immunoreactivity and autoradiography.* (A–D) show a single field. (A) Phase-contrast optics, showing an explant surrounded by migratory cells. (B) Rhodamine optics showing MASH1 immunoreactivity. (C) Fluorescent visualization of the counterstain Hoechst 33258, which labels all nuclei. (D) Bright-field optics showing silver grains deposited over the nuclei of [^{3}H]TdR$^+$ cells. In A, B, and D, arrows show two MASH1$^+$ cells, one of which (large arrow) is [^{3}H]TdR$^+$ and

quired in one particular lineage, that of olfactory receptor neurons.

RESULTS

MASH1-Expressing Cells Are Distinct from Olfactory Receptor Neurons and Keratin$^+$ Basal Cells

Consistent with the idea that MASH1-expressing cells play a role in the generation of ORNs, cells recognized by a monoclonal antibody specific for MASH1 (Lo *et al.*, 1991) could be detected in sections of embryonic mouse OE (Figs. 1A and 1B). To characterize the cell type(s) expressing MASH1, we used a tissue culture system in which OE cells can be identified and their proliferation can be studied.

Briefly, in explant cultures from embryonic day 14.5–15.5 OE, three major cell types are distinguishable by antigenic markers, morphology, and differences in their migratory behavior (Calof and Chikaraishi, 1989; Calof and Lander, 1991; DeHamer *et al.*, 1994): Basal cells (also known as "horizontal" basal cells because they lie directly upon the basal lamina of the OE *in vivo*) express keratin intermediate filaments and do not migrate *in vitro*, instead remaining associated with explanted tissue. Postmitotic ORNs express the neural cell adhesion molecule N-CAM, a neuron-specific marker in this system, and upon appropriate extracellular matrix substrata, migrate away from OE explants and extend neurites (Calof and Lander, 1991; Calof *et al.*, 1994). The third cell type migrates, like ORNs, but is negative for both N-CAM and keratins and is non-neurite-bearing. The vast majority of these latter cells proliferate *in vitro* and give rise to ORNs after one or two rounds of division (Calof and Chikaraishi, 1989; DeHamer *et al.*, 1994); they have therefore been termed immediate neuronal precursors, or INPs. INPs are likely to be the *in vitro* equivalents of "globose" basal cells of the OE (cf. Graziadei and Monti Graziadei, 1979; Mackay-Sim and Kittel, 1991; Schwartz-Levey *et al.*, 1991; Caggiano *et al.*, 1994).

As shown in Figs. 1C and 1D), in OE cultures grown for 10 h, MASH1-immunoreactive cells could readily be detected among the migratory cells, of which they constituted a small fraction (see also Table 1). Similar results were obtained when *Mash1*-expressing cells were detected in OE cultures by nonradioactive *in situ* hybridization (C. S. Stipp and A. L. Calof, unpublished observations). Double-labeling of cultures for MASH1 and either keratins (Figs. 1C, 1E, 1G) or N-CAM (Figs. 1D, 1F, 1H) indicated that migratory, MASH1-expressing cells expressed neither of these two markers: only 2.2 (±1)% of MASH1$^+$ cells showed any keratin immunoreactivity (236 migratory MASH1$^+$ cells counted in two independent cultures), and only 0.5 (±0.5)% showed any N-CAM immunoreactivity (175 MASH1$^+$ cells counted in two independent cultures).

Although the migratory cells in OE cultures include ORNs and INPs, not all ORNs and INPs migrate; some remain associated with explants (Calof and Chikaraishi, 1989). The same was found to be true for MASH1$^+$ cells. Because of the thickness of explants, confocal scanning fluorescence microscopy was required to evaluate the immunoreactivity of MASH1-expressing cells within OE explants. These cells were also essentially negative for both keratins (99 of 102 counted in four independent cultures) and N-CAM (118 of 118 counted in two independent cultures).

Among migratory MASH1$^+$ cells, we noted a morphological distinction: MASH1$^+$ cells often occurred in clusters of 3–10 closely associated cells arrayed in a line or a crescent (Figs. 1G and 1H, black arrows). Although not all MASH1$^+$ cells were in such clusters, the presence of these clusters predicted the presence of MASH1$^+$ cells: If cultures stained with anti-MASH1 were examined first under phase-contrast optics and clusters were chosen solely on the basis of their morphology, 90 (±1)% of clusters were found to contain MASH1$^+$ cells (analyzed in four independent cultures).

MASH1$^+$ Cells Form a Subpopulation of Proliferating Migratory Cells in Olfactory Epithelium Cultures

The characteristics described above for MASH1$^+$ cells are similar to those of INPs, the precursors of ORNs.

one of which (small arrow) is [^{3}H]TdR$^-$. The majority of [^{3}H]TdR$^+$ cells (INPs) do not express MASH1; one of these is marked by an arrowhead. Several MASH1$^+$ cells can be seen to occur as part of closely packed, linear clusters of cells (see text), such as the cluster marked by an asterisk in A and B and the cluster containing the MASH1$^+$ cell marked by the small arrow in A, B, and D. Bar, 25 μm. (E–F) OE explants were cultured for 12 h, with [^{3}H]TdR (0.1 μCi/ml) present throughout the culture period, and processed as in A–D. (E) Rhodamine optics showing a migratory, MASH1$^+$ cell undergoing cytokinesis (arrow). An asterisk shows other MASH1$^+$ cells located at the edge of the explant. (F) The same field as in E, viewed under bright-field optics to show silver grains deposited over [^{3}H]TdR$^+$ cells. The dividing cell illustrated in E (arrow) exhibits silver grains over its two nuclei, indicating that, at some point during the previous 12 h, it incorporated [^{3}H]TdR. Bar, 10 μm.

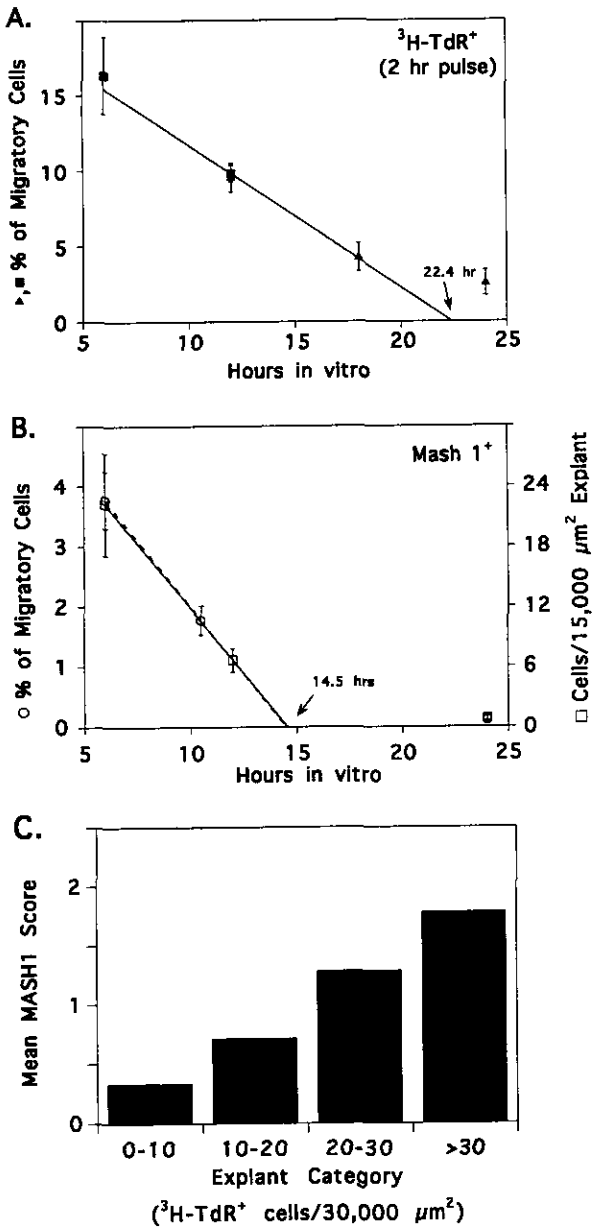

FIG. 3. Analysis of [^{3}H]TdR incorporation and MASH1 expression as a function of time in culture. (A–B) To quantify the disappearance of [^{3}H]TdR-incorporating neuronal precursors and MASH1-expressing cells over the first 24 h *in vitro*, cultures were fixed at various times after plating, with [^{3}H]TdR (5 μCi/ml) present in some during the final 2 h before fixation. (A) For each data point, the percentage of migratory cells (cells that had migrated out from OE explants) that had incorporated [^{3}H]TdR$^+$ was determined for two independent cultures (error bars equal range). Filled triangles and filled squares represent data from two independent experiments. (B) The number of MASH1-expressing cells migrating out from OE explants is expressed using two different indices: As a percentage of total migratory cells (open circles, dashed line) or as an absolute number normalized to explant area (open squares, solid line; the unit of area used in normalizing was 15,000 μm^2, the approximate mean explant area for these tests). Error bars indicate range of values obtained from two independent cultures for each time point. Rates of disappearance of cells in the two populations were estimated from nonlinear least-squares curve-fitting to an equation describing a straight line of negative slope that changes to a straight line of zero slope when it intersects the abscissa. Extrapolated values at Time 0 were 21.1% of migratory cells labeled with [^{3}H]TdR$^+$, 6.4% of migratory cells expressing MASH1, and 37.8 MASH1$^+$ cells/15,000 μm^2 explant. Slopes, relative to their value at Time 0, represented declines of 4.5%/h (A), 6.9%/h (B, open circles), and 6.9%/h (B, open squares). (C) The presence of large numbers of [^{3}H]TdR$^+$ migratory cells surrounding explants in 72-h cultures supplemented with FGF2 (10 ng/ml) was correlated with the presence of MASH1$^+$ cells in those explants. Explants were grown for 72 h and exposed to [^{3}H]TdR (0.1 μCi/ml) during the last 24 h *in vitro*, fixed, and processed for autoradiography and MASH1 immunofluorescence. Eighty-four explants were scored for the number of associated [^{3}H]TdR$^+$ migratory cells. Each explant was also scored for the presence of MASH1$^+$ cells among the migratory cells, associated with the periphery of the explant, or within the body of the explant. In the latter case, an accurate number of MASH1$^+$ cells could not be determined due to explant thickness (which made it difficult to resolve individual cells by fluorescence microscopy), so the bodies of explants were simply scored as positive or negative for MASH1. In the graph shown, each explant along with its associated migratory cells was assigned a "MASH1 score" of 3, 2, 1, or 0 based on whether it had MASH1$^+$ cells in all three locations (among the migratory cells, associated with the periphery of the explant, and within the body of the explant), in two of the three locations, in one of the three locations, or in no location, respectively. The mean MASH1 score was plotted for groups of explants binned according to the number of [^{3}H]TdR$^+$ migratory cells they contained (the sizes of the four bins, from left to right, were 54, 14, 7, and 9 explants, respectively) and demonstrates a positive correlation. Analysis of the raw (unbinned) data yielded a Spearman rank correlation coefficient of 0.61 (Glantz, 1992), indicating statistically significant correlation ($P < 0.001$). Raw [^{3}H]TdR$^+$ labeling data were also plotted with respect to other indices of level of MASH1 expression (number of MASH1$^+$ migratory cells, number of MASH1$^+$ cells either migratory or associated with the periphery of explants) and showed statistically significant positive correlation in each case ($P < 0.01$, data not shown).

INPs are keratin$^-$, N-CAM$^-$, migratory, and non-neurite-bearing. A further distinguishing feature of INPs is that, unlike ORNs (which are postmitotic), they undergo one or more rounds of division *in vitro* (Calof and Chikaraishi, 1989; DeHamer *et al.*, 1994). To determine whether MASH1$^+$ cells are also dividing cells, OE cultures grown for short periods were pulsed with [^{3}H]thymidine ([^{3}H]-TdR) and then fixed and processed for autoradiography and MASH1 immunoreactivity.

As shown in Fig. 2A–2D, in 6-h cultures pulsed for 2 h with [^{3}H]TdR, many MASH1$^+$, migratory cells could be found that were also [^{3}H]TdR$^+$. The data from a series of such pulse-labeling experiments are summarized in Table 1: in cultures pulsed for 2 h with [^{3}H]TdR, the labeling index of MASH1$^+$ cells was 40%; in cultures

labeled for 6 h, the labeling index rose to 80%. That such a high percentage of MASH1$^+$ cells can be labeled with short pulses of [^{3}H]TdR indicates that most, if not all, MASH1$^+$ cells are in the cell cycle (Nowakowski *et al.*, 1989). Furthermore, [^{3}H]TdR-incorporating, MASH1$^+$ cells could occasionally be observed dividing in culture (Figs. 2E and 2F, arrow). Thus, MASH1-expressing cells in OE explant cultures not only proliferate, but continue to express MASH1 through at least M-phase of the cell cycle. Flow cytometric analysis of dissociated cells from OE cultures further indicates that MASH1 is expressed at all stages of the cell cycle (J. S. Mumm and A. L. Calof, unpublished observations).

Although the antigenic properties, motile behavior, and capacity to proliferate of MASH1$^+$ cells match those of INPs, the numbers of MASH1$^+$ cells in OE explant cultures are considerably lower than those of INPs. As shown in Table 1, only about 4.5% of migratory cells are MASH1$^+$. In contrast, at 6 h in culture, INPs make up $\geq$30% of all migratory cells [this is based on data in Table 1, in which 31% of migratory cells were labeled with a 6-h pulse of [^{3}H]TdR, and agrees with data reported previously (Calof and Chikaraishi, 1989; Calof and Lander, 1991; DeHamer *et al.*, 1994)]. Furthermore, regardless of whether cultures were labeled with [^{3}H]TdR for 2 or 6 h, only about 11% of [^{3}H]TdR-incorporating cells were found to express MASH1 (Table 1).

These data, which indicate that MASH1$^+$ cells account for only 10–15% of INPs, could be explained in either of two ways: either INPs are a single cell type, a small fraction of which happen to express MASH1, or MASH1$^+$ cells are a cell type that is functionally distinct from MASH1$^-$ INPs. Data presented in the following sections support the latter view.

MASH1-Expressing Cells Disappear from OE Cultures More Rapidly than INPs

As described previously, most INPs exist only transiently in OE cultures. Their disappearance, which occurs over the first day or two *in vitro*, can be quantitatively accounted for by their division and differentiation into postmitotic, N-CAM$^+$ ORNs (Calof and Chikaraishi, 1989; DeHamer *et al.*, 1994).

Figure 3A follows the disappearance of INPs by plotting the percentage of migratory cells in OE explant cultures that can be pulse-labeled by [^{3}H]TdR as a function of time in culture. The data show a nearly linear loss of INPs, at least for the first 18 h, with a predicted time of disappearance of 22.4 h. In contrast, Fig. 3B plots both the percentages and the numbers of migratory cells in OE explant cultures that are MASH1$^+$ as a function of time in culture. Like the population of INPs as a whole, MASH1$^+$ cells disappear with nearly linear kinetics. However, they do so about 50% more rapidly, with a predicted time of disappearance of 14.5 h. This marked difference provided a first hint that MASH1$^+$ cells may be functionally different from MASH1$^-$ INPs.

In principle, the disappearance of MASH1$^+$ cells could reflect either their differentiation into an antigenically different cell type or their death. The same possibilities apply to the disappearance of INPs as a whole, but previously it has been argued that death is unlikely to account for the disappearance of INPs, both because [^{3}H]-TdR incorporated into INPs can be almost quantitatively "chased" into ORNs and because less than 0.2% of INPs show DNA fragmentation (a characteristic of cells dying by apoptosis) at early times in culture (Calof and Chikaraishi, 1989; DeHamer *et al.*, 1994). In the present study, it was not possible to directly follow the fate of [^{3}H]TdR incorporated into MASH1$^+$ cells (since MASH1$^+$ cells represent only a minority of cells that incorporate the label), but DNA fragmentation was assessed directly: OE explant cultures grown for 10 h were processed for MASH1 immunohistochemistry and for terminal transferase-mediated end-labeling of fragmented DNA (Gavrieli *et al.*, 1992; Holcomb *et al.*, 1995). Of 140 MASH1-expressing cells counted in two independent cultures, only 2.2 $\pm$ 0.8% showed DNA fragmentation. Thus, little evidence for death of MASH1$^+$ cells could be found.

These data suggest that MASH1$^+$ cells disappear from OE cultures primarily by giving rise to MASH1$^-$ cells. This could occur in any of three ways: MASH1$^+$ cells could be giving rise directly to ORNs (as do the bulk of INPs). Alternatively, MASH1$^+$ cells could be the precursors of MASH1$^-$ INPs. Finally, MASH1$^+$ cells could be giving rise to some other, as yet unaccounted for, cell type.

One piece of evidence that favors placement of MASH1$^+$ cells in the ORN lineage (i.e., as precursors of either INPs or ORNs) comes from the analysis of OE explants cultured in the presence of FGF-2 (basic FGF). As previously described (DeHamer *et al.*, 1994), this growth factor has two effects on OE cultures. Over the short term, it increases the number of amplifying divisions that INPs undergo before generating ORNs, although it does not stop the eventual disappearance of INPs from most OE explants and the concomitant cessation of neurogenesis by those explants. Over the longer term, however—3–4 days *in vitro*—a distinct sparing of neurogenesis in a small fraction of OE explants is observed: In the presence of FGF-2, about 5–7% of explants

continue to generate INPs that incorporate [^{3}H]TdR and continue to produce ORNs. These explants can be recognized by their high numbers of [^{3}H]TdR-incorporating cells at late times in culture and may contain a stem cell (which is dependent on FGF for its proliferation and/or survival) that is the ultimate progenitor of ORNs (DeHamer *et al.*, 1994).

If MASH1$^+$ cells play a crucial role in neurogenesis, then one might expect to find FGF-dependent persistence of MASH1$^+$ cells in those explants that show FGF-dependent persistence of neurogenesis. To test this hypothesis, cultures were grown for 3 days in the presence or absence of FGF-2, exposed to [^{3}H]TdR during the last 24 h of culture, fixed, and stained for MASH1. As previously reported, in FGF-2 the numbers of [^{3}H]TdR$^+$ cells per explant (normalized to explant size) did not follow a normal distribution, but showed a significant "tail" of explants with large numbers of proliferative cells (DeHamer *et al.*, 1994). Of the explants analyzed, those with the greatest numbers of proliferative cells (i.e., the top 15th percentile, with a mean of 41 ± 4.3 [^{3}H]TdR$^+$ cells per 30,000 μm^2 of explant area) *all* (100%) had MASH1$^+$ cells either in or immediately surrounding the explant. In contrast, of the remaining explants (exhibiting a mean of 6.7 ± 0.7 [^{3}H]TdR$^+$ cells per 30,000 μm^2 of explant area), MASH1$^+$ cells were detected in only 24%. Interestingly, in the absence of FGF—a condition under which sustained INP production and neurogenesis do not occur (DeHamer *et al.*, 1994)—MASH1$^+$ cells were hardly found at all, appearing in only 2.3% of explants analyzed.

Not only did the presence of MASH1$^+$ cells correlate with the *presence* of sustained INP proliferation, but the relative abundance of MASH1$^+$ cells correlated with the *amount* of INP proliferation. This is demonstrated in Fig. 3C, in which explants were assigned a MASH1 "score" from 0 to 3 that roughly estimates the abundance of MASH1$^+$ cells (see legend). Explants were then binned according the number of [^{3}H]TdR$^+$ cells they possessed (normalized to explant area), and the average MASH1 score was calculated for each bin. A significant positive correlation is evident in the data (Fig. 3C).

Taken together, the data from *in vitro* studies (Figs. 1–3, Table 1) support the idea that MASH1$^+$ cells give rise to INPs. MASH1$^+$ cells are antigenically similar to INPs (i.e., they are keratin$^-$ and N-CAM$^-$), and like them are proliferating cells present in the migratory fraction of OE explant cultures. However, they are present in lower numbers than INPs, and their disappearance precedes that of INPs as neuronal differentiation progresses in culture. Furthermore, under conditions of growth factor supplementation where INPs are found in a fraction of explants at late times in culture, MASH1$^+$ cells are present in the same explants. To gather further evidence to support or refute the idea that MASH1$^+$ cells are progenitors of INPs, as well as to address whether MASH1$^+$ cells are actually the stem cells of the OE, we next turned to *in vivo* experiments.

MASH1 Is Expressed by Proliferating Cells in the Basal Compartment of the Adult OE

If *Mash1* gene activity is required in a precursor of ORNs, then, given that ORN neurogenesis continues throughout life, MASH1-expressing cells should persist throughout life. As shown in Fig. 4, MASH1$^+$ cells are detectable in the adult OE, although they occur much less frequently than in the OE of embryos (Figs. 1A and 1B). In the adult, MASH1$^+$ cells are round cells that lie in the basal compartment of the OE, but not directly adjacent to the basal lamina (Fig. 4A, angled arrows). Counterstaining with the nuclear marker Hoechst 33258 revealed some cases in which MASH1$^+$ cells could be seen lying directly above smaller, flatter cells (the "horizontal" basal cells) that were directly apposed to the basal lamina (Fig. 4C, arrowhead). The morphology and slightly suprabasal location of MASH1$^+$ cells fit the description of the so-called "globose" basal cells (Graziadei and Monti Graziadei, 1979), which are thought to represent the *in vivo* equivalents of INPs (MacKay-Sim and Kittel, 1991; Schwartz Levey *et al.*, 1991). However, counts of MASH1$^+$ cells in the OE of seven different animals suggest that MASH1$^+$ cells are present at a frequency of only 3.9 cells [±1.4 (SEM)] per millimeter of septal OE, sufficiently rare that they could only represent a subpopulation of "globose" basal cells (see below).

Thus, as in embryonic OE cultures, MASH1$^+$ cells in the adult represent a minor population of cells with characteristics similar to INPs. To determine if MASH1$^+$ cells in the adult OE are dividing cells, seven mice were administered sequential pulses of [^{3}H]TdR at 2 and 1 h prior to sacrifice. Cryostat sections of OE were processed for MASH1 immunoreactivity and autoradiography and were counterstained with Hoechst 33258. [^{3}H]-TdR labeling was detected in 39.6 + 4.1% (SEM) of MASH1$^+$ cells, examples of which can be seen in Fig. 4B. It is noteworthy that the labeling index of MASH1$^+$ cells in adult OE is relatively high (suggesting rapid proliferation) and quite comparable to that observed in cultured embryonic OE (cf. Table 1). It is also noteworthy that MASH1$^+$ cells make up only a subset of the dividing cells in the basal compartment of adult OE. Only 10.8% [+ 3.9% (SEM)] of the [^{3}H]TdR$^+$ cells in the

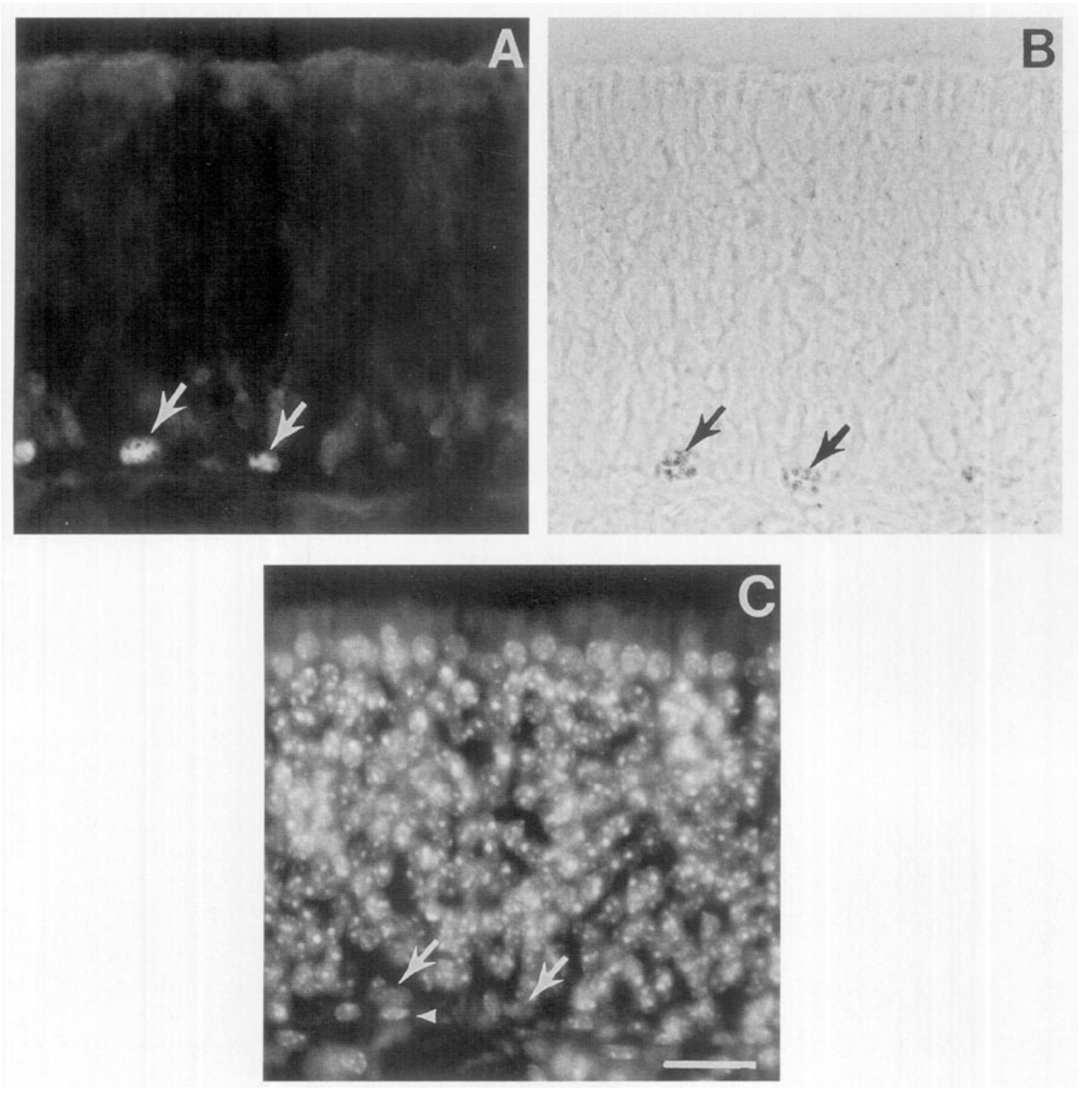

FIG. 4. MASH1-expressing cells are present in the adult OE and incorporate [^{3}H]thymidine. An adult male mouse was given two injections of [^{3}H]thymidine (each 20 μCi/g body wt) at 1-h intervals in the 2-h period prior to sacrifice. Cryostat sections (12 μm) through the olfactory epithelium were processed for MASH1 immunoreactivity and autoradiography and were counterstained with Hoechst 33258. The photos show a single field in which the OE is oriented with its apical surface at the top of the image. (A) Rhodamine optics showing MASH1-expressing cells. (B) Bright-field optics, showing silver grains over nuclei of cells that had incorporated [^{3}H]TdR. (C) Fluorescent visualization of Hoechst 33258 staining of all nuclei. Arrows show two typical MASH1$^+$/[^{3}H]TdR$^+$ cells; they have a rounded morphology and are positioned just above the horizontal basal cell layer. In C, a horizontal basal cell (an elongated cell directly apposed to the basal lamina) is pointed out (arrowhead), to show that an adjacent MASH1$^+$/[^{3}H]TdR$^+$ cell (left arrow) is indeed located above it. Bar, 20 μm.

basal compartment of the OE were MASH1$^+$. Again, these results are quite similar to those obtained with cultured embryonic OE (Table 1). Thus, *in vivo*, MASH1$^+$ cells form a subpopulation of the proliferating cells that have been considered to be the precursors of ORNs (cf. Mackay-Sim and Kittel, 1991; Schwartz Levey *et al.*, 1991). These observations are consistent with the view, suggested by *in vitro* observations, that MASH1$^+$ cells are in the ORN lineage, but are too few in number to be the immediate precursors of ORNs.

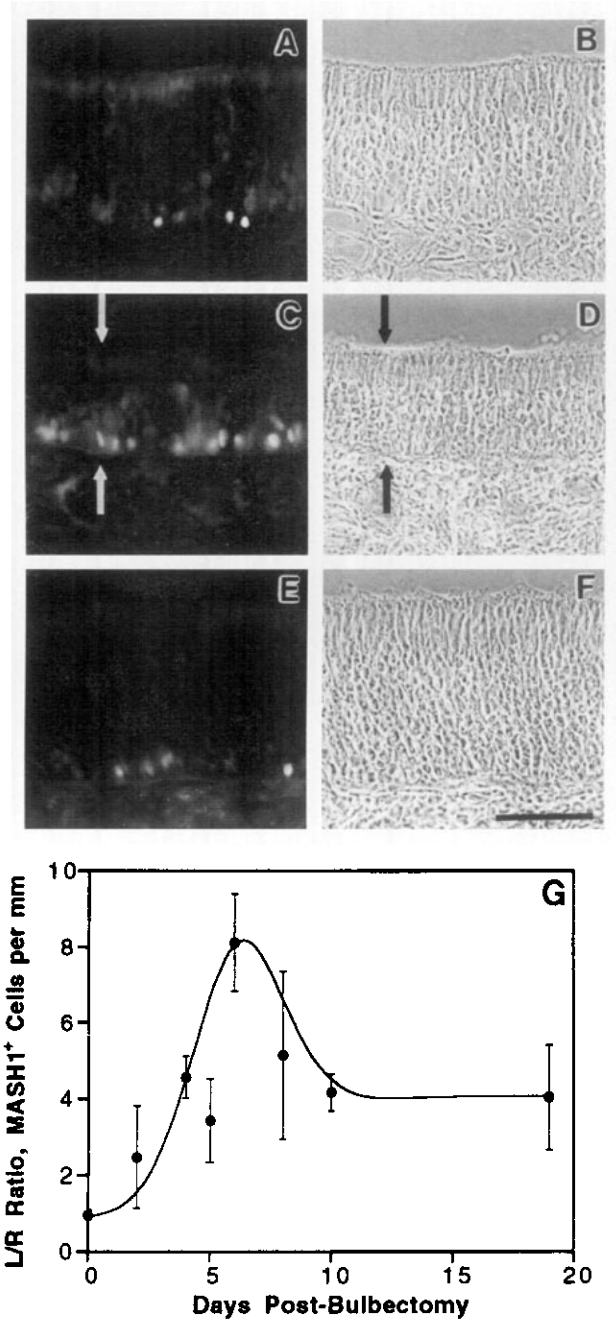

FIG. 5. MASH1-expressing cells increase in number when neurogenesis is stimulated *in vivo*. Adult male mice were subjected to unilateral (left) bulbectomy and sacrificed at various times from 2 to 19 days postsurgery. Several unoperated control animals were also sacrificed. Cryostat sections (12 μm) through the OE were taken in the horizontal plane (so that both left and right OE were present on each section), processed for MASH1 immunoreactivity, and examined by fluorescence and phase-contrast microscopy. (A–F) Photos of the OE of an unoperated animal (A, B) are compared with photos of the left (ipsilateral, operated side; C, D) and the right (contralateral, control side; E, F) septal OE from a single section of an animal sacrificed 5 days after bulbectomy. MASH1 immunofluorescence is shown in A, C, and E; corresponding phase contrast images are shown in B, D, and F. The photos show a marked increase in the number of MASH1$^+$ cells on the ipsilateral side of the operated animal (C), compared to the contralateral (E) or unoperated (A) controls. Also apparent is the decrease in overall thickness of the OE—the results of cell loss—on the ipsilateral side of the operated animal (arrows, C and D), when compared to either of the controls. Bar, 50 μm. (G) Stained sections such as those shown in A–F were used to determine the number of MASH1$^+$ cells per linear distance along the OE on both sides of animals sacrificed at various times following unilateral bulbectomy. To normalize for interanimal variability in the number of MASH1$^+$ cells, data were converted to a ratio of MASH1$^+$ cells/mm on the operated side to MASH1$^+$ cells/mm on the unoperated side, calculated for each animal. The data are plotted as a function of time following bulbectomy. Each data point represents the average of results obtained from at least three animals ± SEM. For each animal, the data were acquired from viewing the OE lying along the posterior part of the nasal septum, in multiple sections, covering several mm of OE. A smooth, freehand curve was drawn through the data points.

When Neurogenesis Is Induced in the OE in Vivo, MASH1$^+$ Cells Undergo a Transient Surge in Number

When one olfactory bulb is surgically ablated in adult rodents (a process known as "bulbectomy"), ORNs in the OE on the side ipsilateral to the lesion die. Degeneration of these cells, accompanied by a decrease in thickness of the OE, is maximal 5–6 days postbulbectomy, a time roughly coincident with a large increase in cell proliferation in the OE. This increase is transient, lasting for 2–3 days, following which new, postmitotic ORNs appear. The newly generated ORNs do not survive long, however (apparently owing to the absence of target tissue), and by 10–14 days postbulbectomy, a new steady state is reached that is different from the preoperative one: Levels of both cell death and cell proliferation are persistently elevated over those seen in unoperated OE, although not as much as during their peaks (Costanzo and Graziadei, 1983; Schwartz-Levey *et al.*, 1991; Carr and Farbman 1992, 1993; Schwob *et al.*, 1992; Holcomb *et al.*, 1995).

We used the bulbectomy paradigm to determine whether numbers of MASH1$^+$ cells in the OE change as a function of the rate of neurogenesis. Adult male mice were subjected to unilateral bulbectomy and sacrificed at intervals from 2 to 19 days postsurgery. Cryostat sections of OE, cut in the horizontal plane, were processed for MASH1 immunoreactivity. In animals sacrificed 4 or more days postbulbectomy, a large increase in MASH1$^+$ cells was observed in the OE ipsilateral to the bulbectomy ("OBX" side), but not in the OE on the control side.

Figure 5 shows examples of MASH1$^+$ cells in the OE of an unoperated animal (A–B), as well as MASH1$^+$ cells in the OE on the OBX side (C–D) and the contralateral, unoperated side (E–F) of an animal sacrificed 5 days postbulbectomy.

To quantify changes in MASH1$^+$ cell number over time during induced neurogenesis, MASH1$^+$ cells were counted in both left (OBX) OE and right (control) OE for several millimeters along the posterior septum for animals sacrificed at 0 (unoperated animals), 2, 4, 5, 6, 8, 10, and 19 days postbulbectomy. The ratio of the number of MASH1$^+$ cells in the OBX versus the control OE was calculated for each animal, and the mean values of these ratios were plotted for each timepoint in Fig. 5G. Following bulbectomy, there is a rapid increase in the number of MASH1$^+$ cells in the OE on the operated side. At the peak, 6 days postbulbectomy, the number of MASH1-expressing cells on the OBX side of an average animal is elevated approximately eightfold over levels on the control side of the same animal. This number then declines, such that by 10 days the elevation is only fourfold, and this new level is maintained for at least 19 days postbulbectomy.

Thus, numbers of MASH1-expressing cells appear to parallel rates of neurogenesis: surging when neurogenesis is abruptly stimulated, and then settling down to a lower, but still elevated, level when neurogenesis returns to a lower, but still elevated level.

Induced Proliferation of MASH1-Expressing Cells Precedes That of INPs

Bulbectomy experiments also provided evidence in support of the idea—already suggested by *in vitro* experiments—that MASH1$^+$ cells precede INPs in the ORN lineage. Bulbectomized animals were pulsed with [^{3}H]-TdR immediately prior to sacrifice, in order to compare proliferation by both the MASH1$^+$ and the MASH1$^-$ cells in the basal compartment of the OE. Briefly, unilaterally bulbectomized mice (bulbectomized 2, 4, 5, 6, 8, or 19 days earlier) and unoperated control animals were given pulses of [^{3}H]TdR at 2 and 1 h prior to sacrifice. Cryostat sections of OE were processed for MASH1 immunoreactivity and autoradiography as in Fig. 4. The numbers of cells in the basal half of the OE that were [^{3}H]TdR$^+$, MASH1$^+$, and doubly positive (MASH1$^+$/[^{3}H]TdR$^+$), were determined for several millimeters of septal OE in each of multiple sections from individual animals; at least three different animals were analyzed for each timepoint.

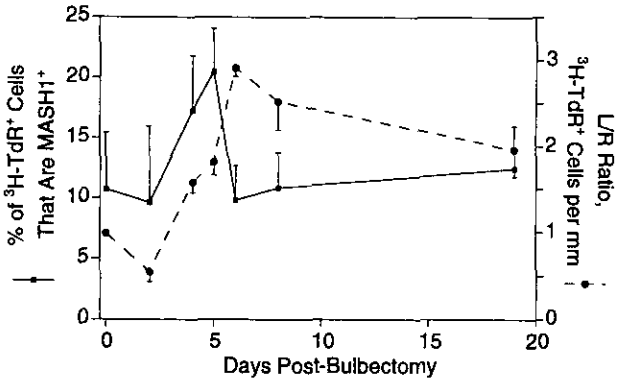

FIG. 6. MASH1$^+$ cells proliferate prior to INPs when neurogenesis is induced *in vivo*. Adult male mice were subjected to unilateral (left) bulbectomy and sacrificed at various times from 2 to 19 days postsurgery. Unoperated control animals were also sacrificed. In all cases, animals were given two sequential injections of [^{3}H]TdR at 2 and 1 h prior to sacrifice, in order to label cells in S-phase with high sensitivity. Cryostat sections (12 μm) were taken and processed as in Fig. 5, except that sections were additionally processed for autoradiography. Data were obtained from counting the number of cells per millimeter of OE that were in the basal half of the epithelium and were MASH1$^+$, had incorporated [^{3}H]TdR, or were both MASH1$^+$ and [^{3}H]TdR$^+$. For each animal, data were collected from several millimeters of septal OE in each of multiple sections, and at least three animals were examined for each time point. The data are presented in two ways: The dashed line shows the number of [^{3}H]TdR$^+$ cells/mm in the OE on the operated (left) side, normalized to the number of [^{3}H]TdR$^+$ cells/mm on the unoperated (right) side. This provides a measure of overall proliferation in the OE on the bulbectomized side. The solid line shows, for the bulbectomized side of each animal, the percentage of [^{3}H]TdR$^+$ cells that is also MASH1$^+$ (calculated for each section examined and averaged over the total number of sections). This provides a measure of the relative contribution of MASH1$^+$ cells to overall proliferation. In both cases, the data points represent means ± SEM. The data indicate that, at early times following bulbectomy, MASH1$^+$ cells contribute preferentially to the increase in overall proliferation, whereas by the time overall proliferation peaks, MASH1$^+$ cells no longer contribute preferentially [note that the value for the percentage of [^{3}H]TdR$^+$ cells that is also MASH1$^+$ at 5 is significantly different from the values at either 0 (P = 0.006) or 6 days (P = 0.001), whereas the values at 0 and 6 days are not significantly different from each other]. Thus, in response to bulbectomy, increased proliferation of MASH1$^+$ cells precedes increased proliferation of cells in the basal half of the OE as a whole (80–90% of which are MASH1$^-$; cf. Fig. 5).

The data are plotted in Fig. 6. The dashed line shows the ratio of the total number of [^{3}H]TdR$^+$ cells per millimeter of OE on the left (OBX) versus the right (unoperated control) side for animals at every time point analyzed. The results indicate that the number of labeled cells increases rapidly in OE on the OBX side, peaks at threefold over the unoperated side at 6 days postsurgery, and then slowly declines. Because horizontal basal cells contribute little to [^{3}H]TdR pulse-labeling of cells in the

basal compartment of the OE in either normal or bulbectomized animals (Schwartz Levey *et al.*, 1991), this curve can be taken as a reflection of overall proliferation in the "globose" basal compartment of the epithelium, i.e., the compartment that includes INPs and MASH1$^+$ cells.

If MASH1$^+$ cells are the progenitors of INPs, then one might expect to see the wave of increased proliferation by (MASH1$^-$) INPs preceded by a wave of proliferation of MASH1$^+$ cells. In contrast, if MASH1$^+$ cells are not the progenitors of INPs, but rather are simply a subpopulation of INPs, then there is no reason to propose that their time course of proliferation should differ from that of other INPs.

A straightforward way to address this question is to measure the fraction of [^{3}H]TdR$^+$ cells (on the OBX side) that is MASH1$^+$ as a function of time following bulbectomy. As stated earlier, this number is approximately 11% in unoperated animals. If, following bulbectomy, MASH1$^+$ cells are preferentially stimulated to divide, then this fraction should rise. Furthermore, if the progeny of MASH1$^+$ cells are INPs, a proliferating cell type that amplifies its own numbers before producing neurons (DeHamer *et al.*, 1994), then this fraction should soon fall again, as an ever greater proportion of the [^{3}H]TdR$^+$ cells are accounted for by MASH1$^-$ INPs. Eventually, a return to a steady-state fraction similar to that observed in unoperated animals should be seen.

The data, shown by the solid line in Fig. 6, exhibit just this behavior. The fraction of [^{3}H]TdR$^+$ cells that is MASH1$^+$ increases quickly, peaks 4–5 days postsurgery (at which point MASH1$^+$ cells account for ~20% of all [^{3}H]TdR$^+$ cells), then declines and remains near unoperated levels by 6–8 days postsurgery. Apparently, bulbectomy induces an early burst of proliferation preferentially in the MASH1$^+$ population. Moreover, this burst precedes the peak of overall proliferation (dashed line) by 1–2 days. Since the data representing overall proliferation primarily reflect proliferation of MASH1$^-$ cells (MASH1$^+$ cells never contribute to more than 20% of the total value), the results indicate that a wave of MASH1$^+$ cell proliferation indeed precedes a wave of proliferation by (MASH1$^-$) INPs.

DISCUSSION

Our current view of the cellular stage in the ORN lineage at which MASH1 acts is diagrammed in Fig. 7. The dynamics of MASH1 expression in the OE suggest that MASH1 expression demarcates a distinct stage of neuronal precursor. Like INPs, MASH1$^+$ cells are keratin-

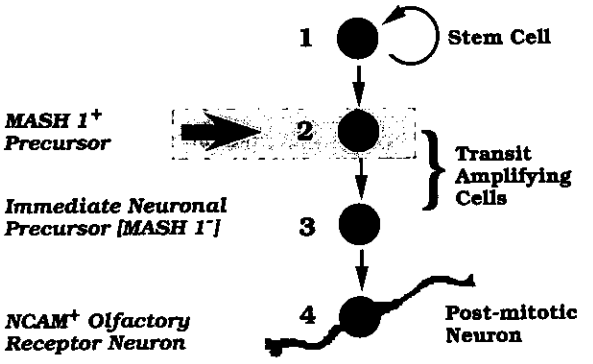

FIG. 7. Proposed model for cellular stages in the olfactory receptor neuron lineage. A model for developmental progression in the olfactory receptor neuron lineage is diagrammed. The stage at which *Mash1* is proposed to act is shown in the shaded box. The model proposes three stages of proliferating neuronal precursor cells in this lineage: a stem cell (as yet unidentified) and two stages of neuronal precursors which act as transit amplifying cells—MASH1-expressing cells and their progeny, the INPs. Olfactory receptor neurons, the progeny of INPs, are postmitotic. Evidence in support of this model is summarized under Discussion.

negative, N-CAM-negative proliferating cells (Figs. 1, 2, and 4), the majority of which are in the cell cycle (Table 1). They differ from INPs in their morphology (they are preferentially found in distinctive cell clusters *in vitro*) and in their numbers [which are 10–15% of that of INPs, both *in vivo* and *in vitro* (Table 1, Fig. 6)].

Under conditions in which rates of ORN neurogenesis are manipulated—*in vitro* and *in vivo*—the numbers and proliferative states of MASH1$^+$ cells and INPs suggest a precursor–product relationship: In OE cultures not supplemented with growth factors, INPs give rise to neurons and are not replaced; under these conditions, MASH1$^+$ cells also disappear, but do so prior to INPs (Figs. 3A and 3B). In OE cultures supplemented with FGF-2, the production of INPs and ORNs is sustained in a fraction of explants; MASH1$^+$ cells are always present in those explants (see text and Fig. 3). In adult animals subjected to unilateral olfactory bulbectomy, proliferation of INPs surges, then drops back to a level still above normal; MASH1$^+$ cell numbers do likewise, but the burst of proliferation of MASH1-expressing cells precedes that of INPs (Figs. 5 and 6).

The proliferative dynamics of MASH1$^+$ cells are characteristic of transit amplifying cells, rather than stem cells. Transit amplifying cells expand their numbers in response to mitogenic stimulation by undergoing rounds of symmetric, or amplifying, divisions; stem cells, as a consequence of their self-renewal, do not undergo substantial changes in number even when stimulated to pro-

liferate, since with every round of division they regenerate, on average, just one copy of themselves (Hall and Watt, 1989; Potten and Loeffler, 1990). The observed surge in the number of MASH1$^+$ cells in the OE following bulbectomy (Fig. 5) clearly fits the expectation for a transit amplifying cell. Furthermore, the high [^{3}H]TdR labeling index of MASH1$^+$ cells in adult OE (~40% labeled by a single 2-h pulse) is also uncharacteristic of stem cells. Typically, stem cells in self-renewing epithelia of adult mammals are very difficult to label with brief pulses of [^{3}H]TdR, owing to their unusually long cell cycle times (e.g., Cotsarelis *et al.*, 1990; Jones *et al.*, 1995).

MASH1 Expression in the OE Suggests That Mash1 Action Is Intrinsic to Neuronal Lineages

From the results of *Mash1* "knockout" experiments in transgenic mice, it can be concluded that MASH1 expression is required, at some time in development, for the production of ORNs (as well as some autonomic and enteric neurons) (Guillemot *et al.*, 1993). However, it is not possible to conclude from such experiments the cell type in which MASH1 action is required. In principle, MASH1 could act at a very early stage in development to set up the ORN lineage, but play no role within the lineage itself thereafter. Or, MASH1 action could be required in cells outside the ORN lineage: For example, MASH1 could act in nonneuronal cells of the OE to regulate their expression of mitogens or trophic factors necessary for proliferation or survival of neuronal precursors and/or ORNs [although *in situ* hybridization experiments have previously demonstrated *Mash1* expression in embryonic OE, cellular localization was not possible with the methods employed in those experiments (Guillemot and Joyner, 1993)]. Finally, the requirement for MASH1 could be intrinsic to the ORN lineage itself.

By localizing MASH1 expression to a specific cell type in the ORN lineage, our data support the third of these possibilities. Furthermore, the novel findings that MASH1$^+$ cells are present in adult OE and during neurogenesis behave similarly to their counterparts in embryonic OE, indicate that the segment of the ORN lineage in which MASH1 is expressed is utilized not only during development, but is continually recapitulated in the adult.

Because the conclusions of the present study are based on the analysis of late embryonic and adult mice, the possibility cannot be ruled out that, in addition to being expressed by the transit amplifying cell described above, MASH1 is also expressed by cell types that have disappeared from the OE by embryonic day 14.5–15.5 (e.g., by early olfactory placode cells that gave rise to the cells of the embryonic OE). Furthermore, even though the present study shows that MASH1$^+$ cells of the OE, on the whole, behave as transit amplifying cells, and not as stem cells, it remains possible that the true stem cell of the OE also expresses MASH1—provided it is sufficiently rare that its contribution to the total MASH1$^+$ population is very small (addressing this possibility awaits identification of a marker for the stem cell). Finally, it should be kept in mind that definitive proof that a gene's action is required in a particular cell type typically requires analysis of genetic mosaics.

Despite these caveats, the present study makes a strong case that MASH1 is expressed—and probably acts—in a lineage-intrinsic manner, at a precise, relatively late (but not the ultimate) precursor stage in the ORN lineage. This view is consistent with results from the study of cultured neural crest cells, in which MASH1 was not expressed by multipotential stem cells, but appeared only after 5–6 days *in vitro*, a time concomitant with neuronal lineage restriction (Shah *et al.*, 1994), and about 3–4 days before the first appearance of neurons (Stemple and Anderson, 1992). Furthermore, results with *CASH1* (the chicken homologue of *MASH1*) also suggest that expression of this transcription factor is associated with a restricted, relatively late stage in retinal neurogenesis (Jasoni *et al.*, 1994).

What Explains the Depletion of ORNs in Mash1$^{-/-}$ Mice?

If MASH1 is expressed at a late step in the ORN lineage, then it follows that the phenotype of nullizygous mice should result from defects in cell behavior at or after that step. For example, the ORN lineage might arrest at the stage when MASH1 is supposed to be expressed. Alternatively, the lineage may go on, but progeny further downstream may adopt abnormal fates, or even die. Recently, we have begun to examine the OE of E14.5–E15.5 *Mash1$^{-/-}$* embryos in an effort to better understand the phenotype. At this stage—a period when normal embryos produce large numbers of N-CAM$^+$ ORNs—the *Mash1$^{-/-}$* OE is abnormally thin and contains very few N-CAM$^+$ cells. N-CAM$^-$ cells are present, however, and these show dramatically elevated levels of cell death, as evidenced by *in situ* detection of DNA fragmentation (M.K.G. and A.L.C., unpublished observations). These results suggest that a substantial number of neuronal precursors are generated in nullizygous animals, but that most of these cells die. Whether it is the cells that were

meant to express MASH1 or their progeny that are dying remains to be determined.

It is noteworthy that in *Mash1*$^{-/-}$ embryos and neonates, the OE is not entirely devoid of ORNs (Guillemot *et al.*, 1993; see above). It could be that there are distinct ORN lineages that do not require MASH1. However, at least as likely is the possibility that the requirement for MASH1 is quantitative, i.e., the probability that an ORN lineage will give rise to neurons is increased by MASH1, but is not zero without it. If MASH1 acts in this way, its role could be to regulate genes that control what a particular neuronal precursor requires for survival within the environment of the OE. By using OE cultures as a source, it may be possible to identify the exogenous factors that regulate the survival of MASH1$^+$ cells and their progeny (cf. DeHamer *et al.*, 1994; Holcomb *et al.*, 1995), and thereby gain insights into signaling pathways upon which MASH1 might act.

Multiple Precursor Stages in the Genesis of Olfactory Receptor Neurons

The scheme outlined in Fig. 7, in which a stem cell gives rise to two successive types of transit amplifying cell—the first MASH1$^+$, the second MASH1$^-$—raises an interesting question: What is the purpose of multiple precursor stages? Unlike neural crest cells, which are multipotential, and for which multiple precursor stages might demarcate progressive restrictions of developmental potential, the neural stem cell of the OE is thought to generate only ORNs, at least in adults (e.g., Caggiano *et al.*, 1994).

One possibility is that multipotentiality exists in the ORN lineage but has not yet been detected. For example, the Schwann-like cells of the olfactory nerve could derive from the same embryonic lineages as ORNs (cf. Chuah and Au, 1991). Furthermore, the recent identification of large families of putative odorant receptor genes, each of which appears to be expressed in subsets of ORNs (Ressler *et al.*, 1993; Vassar *et al.*, 1993), raises the possibility that the selection of particular receptor genes occurs progressively, at specific precursor stages (in this case, one might expect to see similarities in receptor expression among ORNs that are lineally related).

A quite different possibility is that multiple precursor stages in the OE provide multiple control points for the regulation of neurogenesis. For example, each type of precursor may respond to a distinct set of mitogens, survival factors, and differentiation-promoting factors, increasing the number of checkpoints at which neuron production can be controlled. Indeed, the observation that MASH1$^+$ cells in the bulbectomized adult OE undergo increased proliferation before MASH1$^-$ INPs (Fig. 6) strongly suggests that the mitogenic stimuli for INPs and MASH1$^+$ cells are not the same.

EXPERIMENTAL METHODS

Materials

A42B7 hybridoma [mouse anti-MASH1 IgG1 (Lo *et al.*, 1991)] was a kind gift from David Anderson, California Institute of Technology. H28 hybridoma [rat anti-N-CAM IgG (Gennarini *et al.*, 1984)] was a kind gift from Christo Goridis, INSERM–CNRS, Marseilles, France. Recombinant human FGF-2 (basic FGF) was from R&D Systems, and was prepared as a concentrated stock in 1 mg/ml clinical reagent grade bovine serum albumin (BSA; ICN Biochemicals) in calcium- and magnesium-free Hanks' balanced salt solution. [^{3}H]TdR (70–90 Ci/mmol) was from New England Nuclear. NTB2 emulsion, D-19 developer, and fixer were from Kodak. Tissue culture media, antibiotics, and merosin (human) were from Gibco–BRL. Unless otherwise noted, all other reagents were from Sigma.

Tissue Culture

OE was purified as described (Calof and Chikaraishi, 1989) from embryos of CD-1 mice (Charles River) at embryonic day 14.5–15.5 (E14.5–E15.5), where vaginal plug date was designated as E0.5. Explants were cultured as described by DeHamer *et al.* (1994). Briefly, pieces of purified OE were plated onto acid-washed glass coverslips that had been coated with poly-D-lysine and merosin and were cultured in defined, serum-free low calcium culture medium. In some experiments, cultures were supplemented with FGF-2, to a final concentration of 10 ng/ml, added every 24 h. OE coverslip cultures were fixed with 4% paraformaldehyde in 0.02 *M* sodium phosphate, 0.15 *M* NaCl, pH 7.2 (warmed to 37°C). Fixation was for 10 min for double-label immunofluorescence; for 30 min if staining was for MASH1 alone.

Unilateral Olfactory Bulbectomy

Adult male CD-1 mice (4–6 weeks old) were purchased from Charles River and maintained on a 12-h light/12-h dark cycle. Surgeries were generally performed between 10 AM and 2 PM. Anesthesia was obtained via intraperitoneal injection of ketamine (45 mg/

kg) and pentobarbitol (35 mg/kg). The region of the head above the olfactory bulb was shaved with clippers and antisepsis obtained with 70% ethanol. Mice were held in place for surgery with a Stoelting stereotaxic apparatus with mouse adapter. After a midline incision through the scalp, a Dremel drill with diamond-tipped burr was used to expose the left olfactory bulb, which was then aspirated with a No. 3 Baron suction tube. Hemostasis was obtained with gelfoam powder and the scalp was closed with 6-O Ethilon suture. Mice were kept in a warm environment during recovery.

[^{3}H]TdR Labeling

OE cultures were labeled by direct addition of [^{3}H]TdR to culture medium at the times indicated in the text. For a labeling time of 2 h, the final concentration of [^{3}H]TdR was 5 μCi/ml. For a labeling time of 6 h, the final concentration of [^{3}H]TdR was 1 μCi/ml. For a labeling time of 12 h or longer, the final concentration of [^{3}H]TdR was 0.1 μCi/ml. Cells in the OE of live animals were labeled by two intraperitoneal injections of [^{3}H]TdR (each 20 μCi/g body wt) at 2 and 1 h prior to sacrifice.

Tissue Sectioning

Adult male mice were euthanized by lethal overdose of pentobarbitol (ip injection) and perfused with warm (37°C) calcium/magnesium-free Dulbecco's phosphate-buffered saline (PBS) followed by warm 4% paraformaldehyde in 0.02 *M* sodium phosphate, 0.15 *M* NaCl, pH 7.2. The entire nasal vault including the cribriform plate was dissected and postfixed in the same fixative for 1 h at room temperature. Decalcification was carried out for 8–10 days at 4°C in 390 m*M* EDTA, pH 7.1 (modified from Mori *et al.*, 1988). Following decalcification, tissue was equilibrated to 30% sucrose in PBS at 4°C and then sectioned (12 μm) in the transverse (horizontal) plane using a Jung CM 3000 cryostat. Sections were collected on FisherBiotech ProbeOn Plus microscope slides and kept at −20°C until used. E15 mouse embryo heads were fixed for 2–3 h at room temperature in the same paraformaldehyde fixative, then directly equilibrated to 30% sucrose in PBS at 4°C and sectioned as above.

Immunocytochemistry and Autoradiography

Fixed coverslip cultures and tissue sections were blocked and permeablized in 10% calf serum in PBS with 0.2% Triton X-100 for 30 min at room temperature. For single-label immunofluorescent detection of MASH1, undiluted A42B7 hybridoma supernatant was applied overnight at 4°C. After washing with 10% calf serum in PBS with 0.2% Tween, primary antibody was visualized either with rhodamine-conjugated goat anti-mouse IgG (Zymed, 1:30 in 5% goat serum in PBS) or with rabbit anti-mouse IgG1 (Dako, 1:200 in 10% calf serum in PBS) followed by Texas red-conjugated goat anti-rabbit IgG (Jackson Immunoresearch, 1:200 in 5% goat serum in PBS). For double-label immunofluorescence, coverslips or slides were treated either with H28 hybridoma supernatant (anti-N-CAM) or a rabbit antiserum to keratins (Dakopatts Z622; diluted 1:400 in 10% calf serum in PBS) for 7 h at room temperature. After rinsing with 10% calf serum in PBS with 0.2% Tween, biotinylated secondary antibody (Vector rabbit anti-rat IgG for anti-N-CAM staining; Vector goat anti-rabbit IgG for anti-keratin staining) was applied at 2.5 μg/ml in 1 mg/ml crystalline BSA in PBS for 40 min. After rinsing with 1 mg/ml crystalline BSA in PBS plus 0.2% Tween, Zymed FITC Z-avidin (1:50 in 1 mg/ml crystalline BSA in PBS μg/ml) was applied for 30 min. MASH1 was detected as described above, using rhodamine goat anti-mouse IgG as the secondary antibody. Stained coverslips or slides were counterstained with Hoechst 33258 (bisbenzimide, 2 μg/ml) for 10 min to visualize nuclei, then dehydrated and mounted in Protexx (Baxter Scientific). If autoradiography was required, Hoechst staining was omitted, dehydration was followed by air-drying, and coverslips were reverse-mounted onto slides. Slides were dipped in NTB2 emulsion diluted 1:1 in water and exposed at −85°C. Cultures that had been treated with [^{3}H]TdR for 2 or 6 h were exposed for 2 days, cultures treated with [^{3}H]TdR for ⩾12 h were exposed for 7 days, and sections from [^{3}H]TdR-treated animals were exposed for 2 days. After development in D-19 developer, slides were counterstained with Hoechst 33258 and mounted as described above. Specimens were viewed using either a Zeiss axiophot microscope with epifluorescence illumination or a dual laser Bio-Rad MRC-600 confocal scanning unit mounted on a Nikon Optiphot microscope.

Detection of DNA Fragmentation in Vitro

OE cultures were fixed for 10 min at 37°C in 4% paraformaldehyde in 0.02 *M* sodium phosphate with 0.15 *M* NaCl, pH 7.2, permeabilized in PBS with 0.1% Triton X-100, then rinsed twice in TDT buffer (30 m*M* Tris–HCl, 140 m*M* sodium cacodylate, 1 m*M* cobalt chloride, pH 7.2) for 5 min each at room temperature before end-labeling of DNA fragments with biotinylated deoxyuridine triphosphate (TUNEL staining; adapted from Gavrieli *et*

al., 1992) as follows: ~100 μl of reaction mixture [20 μ*M* dUTP and biotin-16-dUTP in a 2:1 ratio in TDT buffer plus 0.2 U/ml terminal transferase (Boehringer Mannheim)] was placed onto the coverslips and incubated for 1 h at 37°C. The reaction was stopped by rinsing in 300 m*M* NaCl, 30 m*M* sodium citrate for 15 min. Coverslips were blocked with 10 mg/ml crystalline BSA in PBS, and biotinylated DNA was detected with FITC-conjugated Z-avidin (Zymed) diluted 1:50 in 1 mg/ml crystalline BSA in PBS.

ACKNOWLEDGMENTS

The authors thank Arthur Lander for many helpful suggestions and comments on the manuscript; Kirk Smith, Mary Burkman, and Jay Guevara for excellent technical assistance; and John Busse for photographic work. This work was supported by grants to A. L. Calof from the Institute on Deafness and Other Communications Disorders of the NIH (DC 02180), the Council for Tobacco Research (3663), and a March of Dimes/Basil O'Connor Scholar Award.

REFERENCES

Blaugrund, E., Pham, T. D., Tennyson, V. M., Sommer, L., Anderson, D. J., and Gershon, M. D. (1994). Multiple lineages in the development of the enteric nervous system (ENS): Selective failure of the differentiation of serotonergic neurons in mice with a homozygous disruption of the mammalian *achaete-scute* homologue (Mash1). *Soc. Neurosci. Abstr.* **20:** 654.

Caggiano, M., Kauer, J. S., and Hunter, D. D. (1994). Globose basal cells are neuronal progenitors in the olfactory epithelium: A lineage analysis using a replication-incompetent retrovirus. *Neuron* **13:** 339–352.

Calof, A. L. (1995). Intrinsic and extrinsic factors regulating vertebrate neurogenesis. *Curr. Opinion Neurobiol.* **5:** 19–27.

Calof, A. L., and Chikaraishi, D. M. (1989). Analysis of neurogenesis in a mammalian neuroepithelium: Proliferation and differentiation of an olfactory neuron precursor in vitro. *Neuron* **3:** 115–127.

Calof, A. L., and Lander, A. D. (1991). Relationship between neuronal migration and cell-substratum adhesion: Laminin and merosin promote olfactory neuronal migration but are anti-adhesive. *J. Cell Biol.* **115:** 779–794.

Calof, A. L., Campanero, M. R., O'Rear, J. J., Yurchenco, P. D., and Lander, A. D. (1994). Domain-specific activation of neuronal migration and neurite outgrowth-promoting activities of laminin. *Neuron* **13:** 117–130.

Camara, C. G., and Harding, J. W. (1984). Thymidine incorporation in the olfactory epithelium of mice: Early exponential response induced by olfactory neurectomy. *Brain Res.* **308:** 63–68.

Campos-Ortega, J. A. (1993). Mechanisms of early neurogenesis in *Drosophila melanogaster*. *J. Neurobiol.* **24:** 1305–1327.

Campos-Ortega, J. A., and Jan, Y. N. (1991). Genetic and molecular basis of neurogenesis in *Drosophila melanogaster*. *Annu. Rev. Neurosci.* **14:** 399–420.

Campuzano, S., and Modolell, J. (1992). Patterning of the *Drosophila* nervous system: The *achaete–scute* gene complex. *Trends Genet.* **8:** 202–208.

Carr, V. M., and Farbman, A. I. (1992). Ablation of the olfactory bulb up-regulates the rate of neurogenesis and induces precocious cell death in olfactory epithelium. *Exp. Neurol.* **115:** 55–59.

Carr, V. M., and Farbman, A. I. (1993). The dynamics of cell death in the olfactory epithelium. *Exp. Neurol.* **124:** 308–314.

Chuah, M. I., and Au, C. (1991). Olfactory Schwann cells are derived from precursor cells in the olfactory epithelium. *J. Neurosci. Res.* **29:** 172–180.

Costanzo, R. M., and Graziadei, P. P. C. (1983). A quantitative analysis of changes in the olfactory epithelium following bulbectomy in hamster. *J. Comp. Neurol.* **215:** 370–381.

Cotsarelis, G., Sun, T.-T., and Lavker, R. M. (1990). Label-retaining cells reside in the bulge areo of pilosebaceous unit: Implications for follicular stem cells, hair cycle, and skin carcinogenesis. *Cell* **61:** 1329–1337.

DeHamer, M. K., Guevara, J. L., Hannon, K., Olwin, B. B., and Calof, A. L. (1994). Genesis of olfactory receptor neurons in vitro: Regulation of progenitor cell divisions by fibroblast growth factors. *Neuron* **13:** 1083–1097.

Gavrieli, Y., Sherman, Y., and Ben-Sasson, S. A. (1992). Identification of programmed cell death in situ via specific labeling of nuclear DNA fragmentation. *J. Cell Biol.* **119:** 493–501.

Gennarini, G., Rougon, G., Deagostini-Bazin, H., Hirn, M., and Goridis, C. (1984). Studies on the transmembrane disposition of the neural cell adhesion molecule NCAM. *Eur. J. Biochem.* **142:** 57–64.

Glantz, S. A. (1992). *Primer of Biostatistics*, 3rd ed. McGraw-Hill, New York.

Graziadei, P. P. C., and Monti Graziadei, G. A. (1978). Continuous nerve cell renewal in the olfactory system. In *Handbook of Sensory Physiology, Vol. IX, Development of Sensory Systems* (M. Jacobson, Ed.), pp. 55–83. Springer-Verlag, New York.

Graziadei, P. P. C., and Monti Graziadei, G. A. (1979). Neurogenesis and neuron regeneration in the olfactory system of mammals. I. Morphological aspects of differentiation and structural organization of the olfactory sensory neurons. *J. Neurocytol.* **8:** 1–18.

Greenspan, R. J. (1992). Initial determination of the neurectoderm in *Drosophila*. In *Determinants of Neuronal Identity* (M. Shankland and E. R. Macagno, Eds.), pp. 155–188. Academic Press, San Diego.

Guillemot, F., and Joyner, A. L. (1993). Dynamic expression of the murine *achaete–scute* homologue *Mash-1* in the developing nervous system. *Mech. Dev.* **42:** 171–185.

Guillemot, F., Lo, C.-C., Johnson, J. E., Auerbach, A., Anderson, D. J., and Joyner, A. L. (1993). Mammalian achaete-scute homolog 1 is required for the early development of olfactory and autonomic neurons. *Cell* **75:** 463–476.

Guillemot, F., Nagy, A., Auerbach, A., Rossant, J., and Joyner, A. L. (1994). Essential role of Mash-2 in extraembryonic development. *Nature* **371:** 333–336.

Hall, P. A., and Watt, F. M. (1989). Stem cells: The generation and maintenance of cellular diversity. *Development* **106:** 619–633.

Holcomb, J. D., Mumm, J. S., and Calof, A. L. (1995). Apoptosis in the neuronal lineage of the mouse olfactory epithelium: Regulation in vivo and in vitro. *Dev. Biol.*, in press.

Jasoni, C. L., Walker, M. B., Morris, M. D., and Reh, T. A. (1994). A chicken *achaete–scute* homolog (*CASH-1*) is expressed in a temporally and spatially discrete manner in the developing nervous system. *Development* **120:** 769–783.

Johnson, J. E., Birren, S. J., and Anderson, D. J. (1990). Two rat homologues of *Drosophila achaete–scute* specifically expressed in neuronal precursors. *Nature* **346:** 858–861.

Jones, P. H., Harper, S., and Watt, F. M. (1995). Stem cell patterning and fate in human epidermis. *Cell* **80:** 83–93.

Lo, L.-C., Johnson, J. E., Wuenschell, C. W., Saito, T., and Anderson, D. J. (1991). Mammalian achaete–scute homolog 1 is transiently expressed by spatially restricted subsets of early neuroepithelial and neural crest cells. *Genes Dev.* **5:** 1524–1537.

Mackay-Sim, A., and Kittel, P. (1991). Cell dynamics in the adult mouse olfactory epithelium: A quantitative autoradiographic study. *J. Neurosci.* **11:** 979–984.

Monti Graziadei, G. A., and Graziadei, P. P. C. (1979). Neurogenesis and neuron regeneration in the olfactory system of mammals. II. Degeneration and reconstitution of the olfactory sensory neurons after axotomy. *J. Neurocytol.* **8:** 197–213.

Mori, S., Sawai, T., Teshima, T., and Kyogoku, M. (1988). A new decalcifying technique for immunohistochemical studies of calcified tissue, especially applicable to cell surface marker demonstration. *J. Histochem. Cytochem.* **36:** 111–114.

Nowakowski, R. S., Lewin, S. B., and Miller, M. W. (1989). Bromodeoxyuridine immunohistochemical determination of the lengths of the cell cycle and the DNA-synthetic phase for an anatomically defined population. *J. Neurocytol.* **18:** 311–318.

Potten, C. S., and Loeffler, M. (1990). Stem cells: Attributes, cycles, spirals, pitfalls and uncertainties. Lessons for and from the crypt. *Development* **110:** 1001–1020.

Ressler, K. J., Sullivan, S. L., and Buck, L. B. (1993). A zonal organization of odorant receptor gene expression in the olfactory epithelium. *Cell* **73:** 597–609.

Schwartz Levey, M., Chikaraishi, D. M., and Kauer, J. S. (1991). Characterization of potential precursor populations in the mouse olfactory epithelium using immunocytochemistry and autoradiography. *J. Neurosci.* **11:** 3556–3564.

Schwob, J. E., Mieleszko Szumowski, K. E., and Stasky, A. A. (1992). Olfactory sensory neurons are trophically dependent on the olfactory bulb for their prolonged survival. *J. Neurosci.* **12:** 3896–3919.

Shah, N. M., Marchionni, M. A., Isaacs, I., Stroobant, P., and Anderson, D. J. (1994). Glial growth factor restricts mammalian neural crest stem cells to a glial fate. *Cell* **77:** 349–360.

Stemple, D. L., and Anderson, D. J. (1992). Isolation of a stem cell for neurons and glia from the mammalian neural crest. *Cell* **71:** 973–985.

Vassar, R., Ngai, J., and Axel, R. (1993). Spatial segregation of odorant receptor expression in the mammalian olfactory epithelium. *Cell* **74:** 309–318.

Received for publication June 29, 1995